NUMERICAL ANALYSIS BY VIRTUAL TESTING REPLACING EXPERIMENTS WITH TENSION ROD SYSTEMS

Albrecht Gehring [1,*], Richard Goodman [2], Helmut Saal [3] and Chris Willett [4]

[1] *Engineering consultant, Lauer & Weiss GmbH, Höhenstraße 21, 70736 Fellbach, Germany*
[2] *Engineering design manager, Macalloy Limited, Caxton Way, Dinnington, S25 3QE, United Kingdom*
[3] *Professor, Versuchsanstalt für Stahl, Holz und Steine, Universität Karlsruhe (TH), Germany*
[4] *Sales director, Macalloy Limited, Caxton Way, Dinnington, S25 3QE, United Kingdom*
[*] *(Corresponding author: E-mail: albrecht.gehring@lauer-weiss.de)*

Received: 31 January 2007; Revised: 22 August 2007; Accepted: 4 September 2007

ABSTRACT: The resistance of tension rod systems can be calculated according to design codes, e.g. Eurocode 3 or DIN 18800-1. Often the real load bearing capacity is not activated by the calculated resistance – which is due to a conservative approach of the analytical design methods. The real load bearing capacity of the whole system can be evaluated by a series of ultimate load tests. The results of these tests lead to technical approvals. This procedure takes a lot of time and is very cost intensive. Therefore some European building authorities are allowing virtual tests to reduce both costs and time. A general strategy for preparing and performing virtual tests of tension rod systems is presented in this paper. Special attention is paid to generate a clear numerical model with respect to possible failure modes. The application of this strategy is illustrated by an example of virtual tests which led to a technical approval in Germany.

Keywords: Tension rod system; finite-element analysis; virtual testing; failure criteria; static resistance

1. INTRODUCTION

Modern sophisticated steel structures are unthinkable without the application of tension rod systems. They are applied as bracing for buildings or beams and in bridges. The first ever structure built with tension rod systems is shown on Figure 1. Commissioned as a distribution facility, the Renault Centre was designed to maximise internal flexibility. The repeated structural system makes use of tension rods, which support the roof structure. Stainless steel tension rods are used to support the bridge deck from a tubular steel arch or the flamboyant roof structure from large steel arches, see Figure 1 and Figure 2. Tension rods are used to support the roof trusses and skylights, see Figure 3. The roof of the Sazka arena shown on Figure 4 takes the shape of a spherical cap spanning 135m and with a rise of 9m. It is supported by a pre-stressed space beam tension rod structure. Other applications are described in Kathage et al. [1].

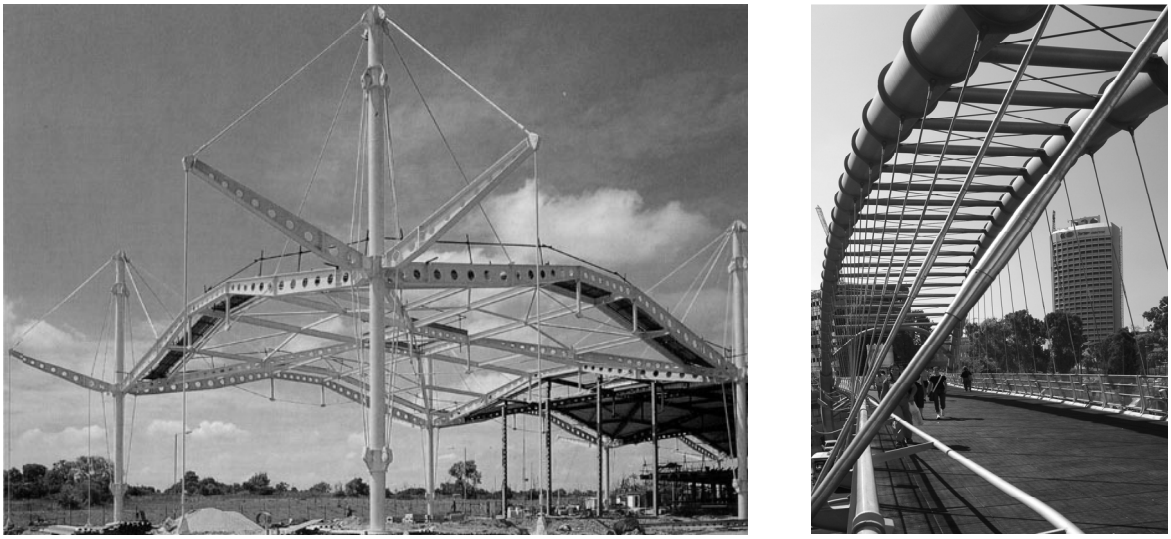

Figure 1. Renault Distribution Centre, Swindon, UK, 1983 (left)
Pedestrian Bridge, Tel Aviv, Israel, 2005 (right)

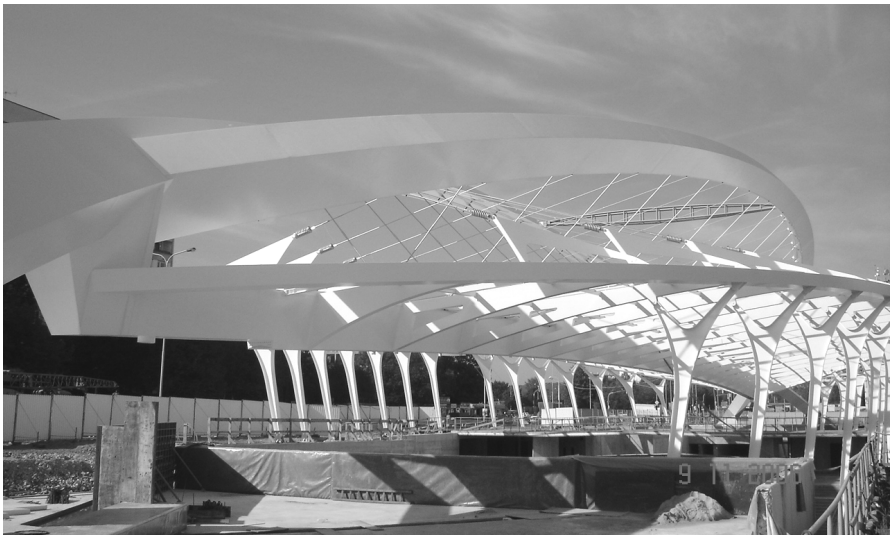

Figure 2. Metro station, Stritzkov, Prague, Czech Republic. 2005

Figure 3. Ports International Airport, Porto, Portugal. 2005

Figure 4. Sazka Arena, Prague, Czech Republic. 2004

Often conservative results are obtained by a calculation of the resistance of a tension rod system according to the European standards EN 1993-1-1 [2] and EN 1993-1-8 [3] or the German standard DIN 18800-1 [4], [5]. This leads to uneconomic building components. The actual load bearing capacity could be utilised by an assignment of a technical approval which is based on extensive tests. A Common Understanding of Assessment Procedure CUAP [6] regulates the test procedures and the number of tests in Europe. This procedure takes a lot of time and is cost intensive. Therefore some European building authorities [7], Breitschaft and Häusler [8], Kathage [9] are allowing virtual tests to reduce both costs and time. The strategy, performance and verification of virtual tests is exemplified below with a tension rod system. The results of the example, Saal and Gehring [10], led to an assignment of a technical approval [11] in Germany.

2. COMPONENTS AND DESIGN METHODS

A tension rod system usually consists of several components, Figure 6. The fork end connectors are fabricated from steel by casting or forging. Usually high strength steel grades are utilised for the pins, Kathage et al. [1]. The tension rods are executed in steel grades up to S690. Couplers, turnbuckles and circular gusset plates complement standard tension rod systems. The tension rod is joint to the structure by a single bolted connection between a fork end connector and an end plate.

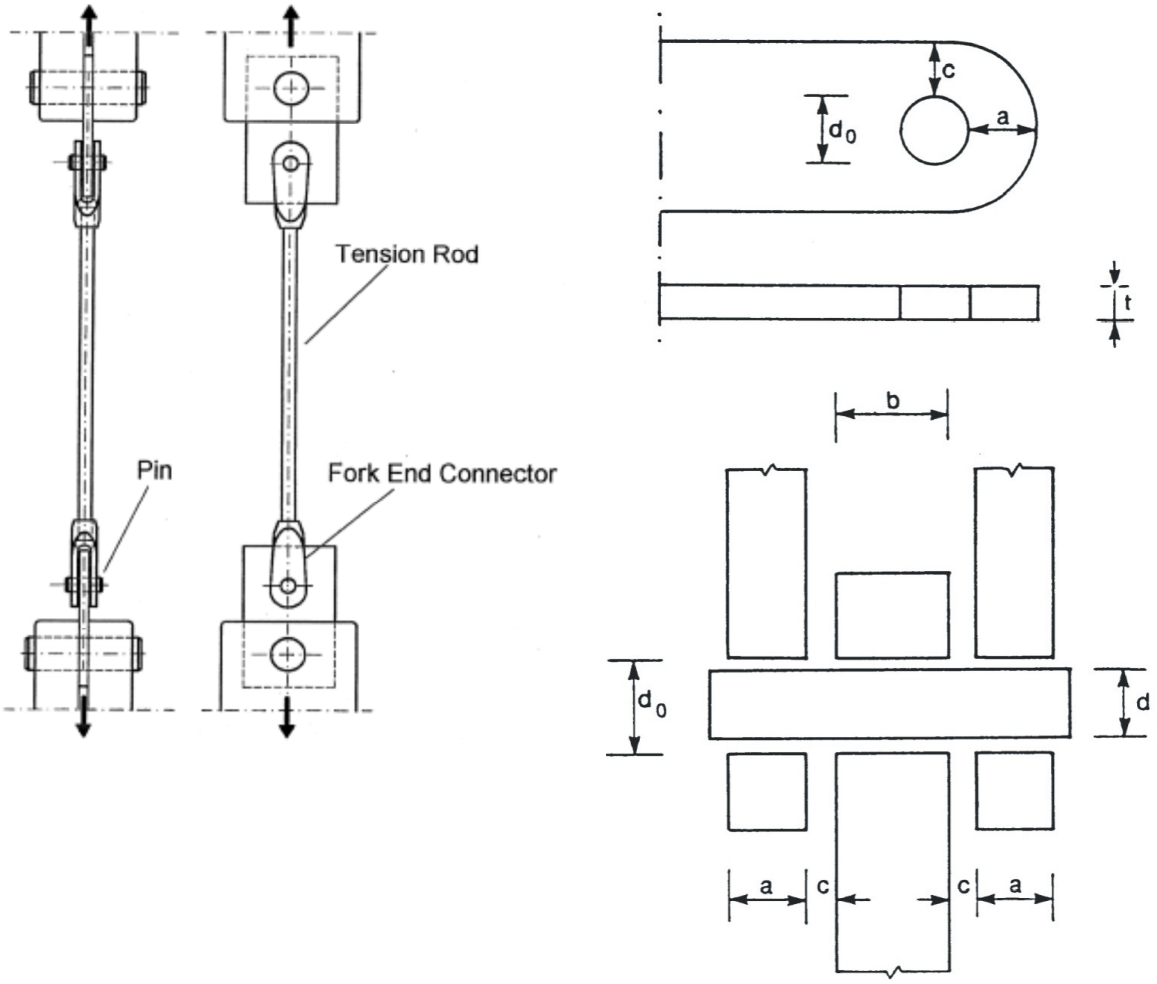

Figure 6. General Assembly of a Tension Rod System (left, from [6]) and Notation for Fork End Connector (right, top) and Pin (right, bottom), Both from [3]

The design of all components is usually performed according to Eurocode 3 [2, 3] or DIN 18800-1 [4, 5]. The resistance of the threaded connection of the tension rod to the fork end connector may be calculated according to VDI-Richtlinie 2230 [12] up to size M 100. The design methods are explained in detail in Kathage et al. [1].

With the notation of Eurocode 3 [2], [3] see Figure 6, the characteristic resistance $F_{fec,c}$ of a fork end connector is obtained according to German standards DIN 18000-1 [4], [5] from the formulae

$$F_{fec,c} = \min \begin{cases} F_{fec,1,c} = (a - 2/3\, d_0)\; 2\; t\; f_{y,fec}\; 2 \\ F_{fec,2,c} = (c - 1/3\, d_0)\; 2\; t\; f_{y,fec}\; 2 \\ F_{fec,3,c} = t\; d\; 1{,}5\; f_{y,fec}\; 2 \end{cases} \tag{1}$$

and the characteristic resistance $F_{pin,c}$ of the pin is obtained from

$$F_{pin,c} = \min \begin{cases} F_{pin,1,c} = 0{,}6\; A\;\; f_{up}\; 2 \\ F_{pin,2,c} = \dfrac{8\; f_{yp}\; W_{el}}{1{,}25\; (b + 4\; c + 2\; a)} \end{cases} \tag{2}$$

where W_{el} is the elastic section modulus of the pin. In addition the interaction of bending moment and shear forces has to be examined.

The characteristic resistance $F_{tr,c}$ of the tension rod is obtained from German standards DIN 18000-1 [4], [5] as

$$F_{tr,c} = \min \begin{cases} F_{tr,1,c} = \dfrac{f_{yb}}{1{,}1}\; A \\ F_{tr,2,c} = \dfrac{f_{ub}}{1{,}25}\; A_s \end{cases} \tag{3}$$

which is slightly different from European standards [2, 3]. In Eq. 3 A is the gross cross section and A_s is the tensile stress area of the tension rod.

Usually the resistance of the whole system is limited by the load bearing capacity of the pin according to Eq. 2. This is due to a conservative approach, which does not take into account the real load transfer, Kathage et al. [1]. A comparison of the assumed uniform distribution of the reactions between pin and fork end and their real distribution is given in Saal and Bechtold [13].

For safety purposes it is desirable that the load bearing capacity of a tension rod system is governed by that of the tension member. In this case it has to be guaranteed that the resistance of fork end connector, pin, coupler etc. exceeds the resistance of the tension member. This can be demonstrated by conservative formulae, e.g. Eq. 1 and Eq. 2, or by tests. This latter procedure is the basis for technical approvals for individual tension rod systems where the design is reduced to the application of Eq. 3, Kathage et al. [1].

3. EXECUTION OF VIRTUAL TESTS

Virtual tests will only lead to safe results if they are based on a profound knowledge of the load transfer and the possible failure modes. This demands substantial experience with experimental and numerical analysis of the object. This has to be kept in mind for safety reasons when virtual tests are performed.

In general, the performance of virtual tests can be divided in the following sub-steps:

- Determination of characteristic resistances of all components according to European [2, 3] or German [4, 5, 12] standards.
- Estimation of results in order to simplify the numerical model such that only relevant failure modes are included
- Generation of a numerical model: geometry, material laws, contact conditions
- Theoretical verification of the model: proof of plausibility of the failure modes (shear failure, bending failure of pin, etc.) and derivation of failure criteria.
- Experimental verification of the model and the failure criteria: comparison of failure loads obtained numerically and experimentally.
- Performance of virtual tests with the verified model. The failure loads are obtained by application of the derived failure criteria.

A mechanically reasonable model is obtained by application of the first two steps. Economic design rules should be applied if available, e.g. VDI-Richtlinie [12]. The numerical model can be simplified with this, because these failure modes must not be analysed in the virtual tests. Thus, the attention can be focused on the interesting load transfer mechanisms and failure modes. Unlike Kathage et al. [1], we recommend to generate separate numerical sub-models for analysis of the different failure modes. This separation allows a target-oriented fine mesh for the numerical model and a clear interpretation of the results. The failure modes are assessed by the application of mechanical considerations and present experiences. The ultimate failure loads are determined with well defined failure criteria. The quality of the failure criteria has to be verified experimentally. Then, all necessary virtual tests can be performed with the verified numerical model. If the results obtained by the virtual tests physically make no sense, experimental investigations are unavoidable for safety reasons.

4. EXAMPLE

4.1 Components and Limitations

All steps of the virtual tests are explained by an example, Saal and Gehring [12]. In this case a German technical approval [11] for a tension rod system was extended for sizes M85, M90 and M100 by the results of virtual tests. This tension rod system is shown in Figure 7 schematically. The relevant dimensions are listed in Table 1.

The characteristic resistances calculated with Eq. 1 to Eq. 3 are given in Table 4. The characteristic resistance $F_{VDI,c}$ of the threaded connection between fork end connector and tension rod given in Table 4 was calculated according to VDI-Richtlinie 2230 [13]. This was confirmed in many previous tests with connections of that type as a safe and economic approach. Because of this the thread need not be modelled.

Table 1. Dimensions of the Tension rod System

	M20	M30	M76	M85	M90	M100
	mm	mm	Mm	mm	mm	Mm
d_{sp}	17	25	67	77	82	92
A	122	178	410	459	489	555
B	51	79	199	236	248	289
C	29	43	108	121	129	143
D	15	22	70	70	80	85
E	24	32	78	87	92	102
G	19	26	76	79	87	92
H	37	48	148	153	169	174
K	21	31	78	91.5	96.5	111.5
N	20	30	76	90	93	108
T	9	11	36	37	41	41
V	33	52	131	153	162	188

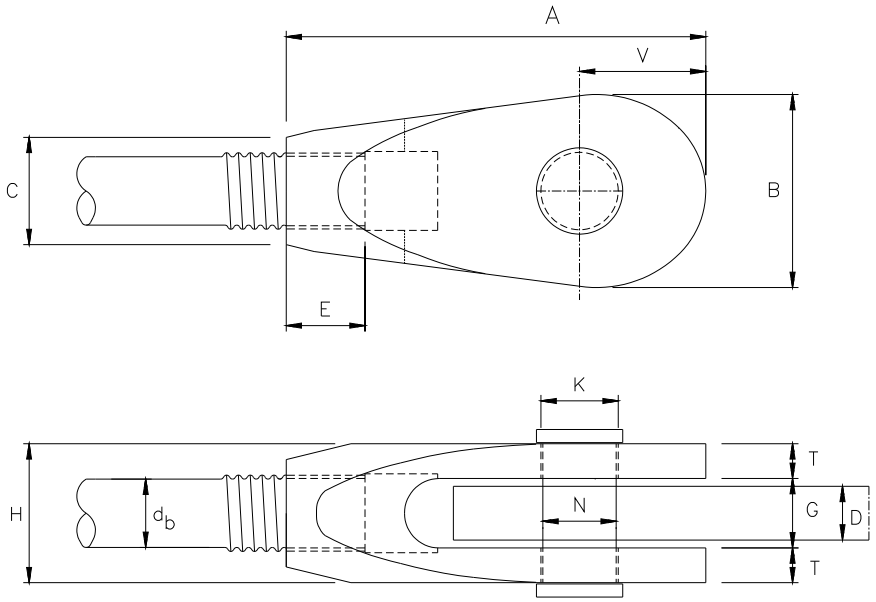

Figure 7. Schematic Drawing of Tension rod System, From [11]

4.2 Description of Numerical Model

The virtual tests are performed with the commercial Finite-Element package ABAQUS/Standard [14]. The single components fork end connector, pin and end plate are modelled. Due to the double symmetry, the finite-element model represents a quarter of the structure. The end of the fork end connector is modelled with parallel surfaces instead of the tapering. This has no effect on the load bearing capacity for which only the pin and the neighbouring area of the fork end is relevant. The end plate is represented by rigid elements for the same reason. A contact without friction is defined between fork end connector and pin. This assumption is based on test results, Saal and Gehring [10].

The end plate is defined as fixed support. The load is applied by a translation of the threaded area in 2-direction, see Figure 8. The fork end connector and the pin are meshed with continuum element type C3D8R, Abaqus [15]. The analysis is performed with the finite-element mesh shown in Figure 8.

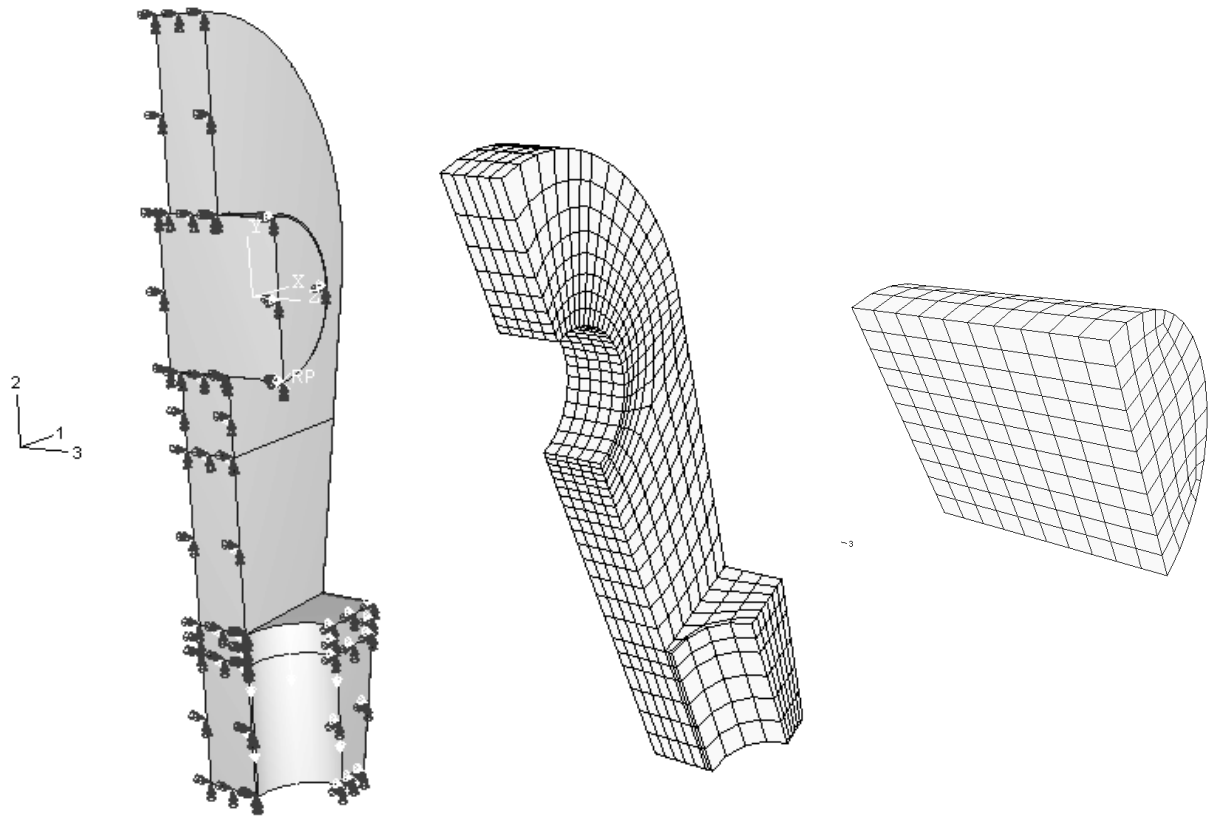

Figure 8. Boundary Conditions, Meshed Fork end Connector and Pin

The material behaviour is described by a bi-linear isotropic material law for both the fork end connector and the pin. Plastic deformations are controlled by the von-Mises yield criterion with an associated flow rule. The material is characterised by the yield strength f_y and the tensile strength f_u. The nominal stresses σ and strains ε are transformed into true stresses σ_{true} and true strains ε_{true} for all calculations with

$$\sigma_{true} = \sigma\,(1+\varepsilon) \tag{4}$$

$$\varepsilon_{true} = \ln\,(1+\varepsilon) \tag{5}$$

This gives a realistic deformation response for the ultimate failure load which is determined by the tensile strength.

The nominal material properties are taken from a technical approval [11]. The material parameters used for the analyses are given in Table 2.

Table 2. Material Parameters

	Elastic constants *		Point A **		Point B ***	
	E	ν	σ_{true}	ε_{true}	σ_{true}	ε_{true}
	GPa	-	MPa	-	MPa	-
Fork end connector	210	0.3	335	0.00	660	0.095
Pin	210	0.3	640	0.00	854	0.065

* Young's modulus E and Poisson's ratio ν
** Stress and plastic strain at yield point
*** Stress and plastic strain at failure

4.3 Derivation of a Failure Criteria

A failure criterion is derived from the design rules for the net section of tension members. According to Anpassungsrichtlinie [5] the ultimate limit state is controlled by the tensile strength without limitation of plastic strains. However, for the virtual ultimate failure load $F_{FEM,u}$ of the fork end connector this criterion is extended by a limitation of the plastic strain ε_{pl} to the ultimate value ε_{true}. Thus

$$F_{FEM,u} = F_{FEM}(\varepsilon_{pl}) \tag{6}$$

where $\varepsilon_{pl} = \max(\varepsilon_{EPPQ}, \varepsilon_{PE22}) < \varepsilon_{true}(A_g)$ and A_g is the uniform elongation.

The plastic strain ε_{pl} is obtained from the numerical calculations as the maximum of equivalent plastic strain ε_{EPPQ} and the plastic strain ε_{PE22} in direction of loading. The equivalent plastic strain accounts for the triaxial stress state. Tension stresses close to the hole are represented by the plastic strain in the direction of loading. The ultimate failure load is attained, when the plastic strain ε_{pl} equals $\varepsilon_{true}(A_g)$. This means, the tensile strength is reached locally in contrast to the design rules for the net section of tension members.

In this example the pin is not controlling the ultimate failure load of the tension rod system because the tensile strength of the fork end connector is much less than the yield strength of the pin.

4.4 Experimental Verification

The finite-element model is verified with the results of existing ultimate load tests obtained for different system sizes. The comparative calculations are performed with the measured geometries and material data from the tests. The ultimate failure loads of the virtual tests are determined by application of the failure criterion Eq. 6. The failure loads determined numerically with this criterion are compared to the experimental results in Table 3.

A fork end connector size M 76 in the ultimate limit state according to Eq. 6 is shown in Figure 9 with the distribution of the equivalent plastic strain and plastic strain in direction of loading. An example of a broken fork end connector is shown in Figure 10. The collapse was initiated by a tensile failure of one plate of the fork end connector. The following dynamic process leads to the visible bending of the other plate. Plastic deformations did not occur in the pin and the end plate.

Table 3. Verification of the Numerical Model by Comparison of Numerical and Experimental Failure Loads

Size	Virtual test $F_{FEM,u}$	Real test F_{Exp}	Difference
	kN	kN	%
M 20	243	272	-10.1
M 30	506	505	+0.2
M 76	3778	3816	-1.0

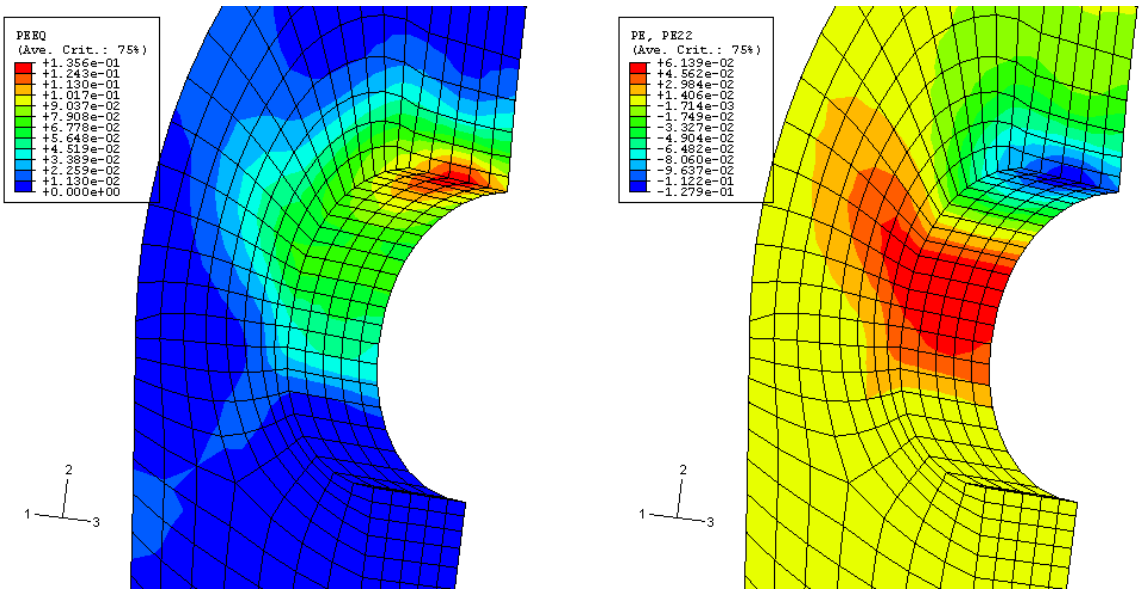

Figure 9. Equivalent Plastic Strain (Top) and Plastic Strain in Direction of Loading (Bottom) at Ultimate Limit State According to Failure Criteria (6)

Figure 10. Broken Fork End Connecter after Ultimate Load Test

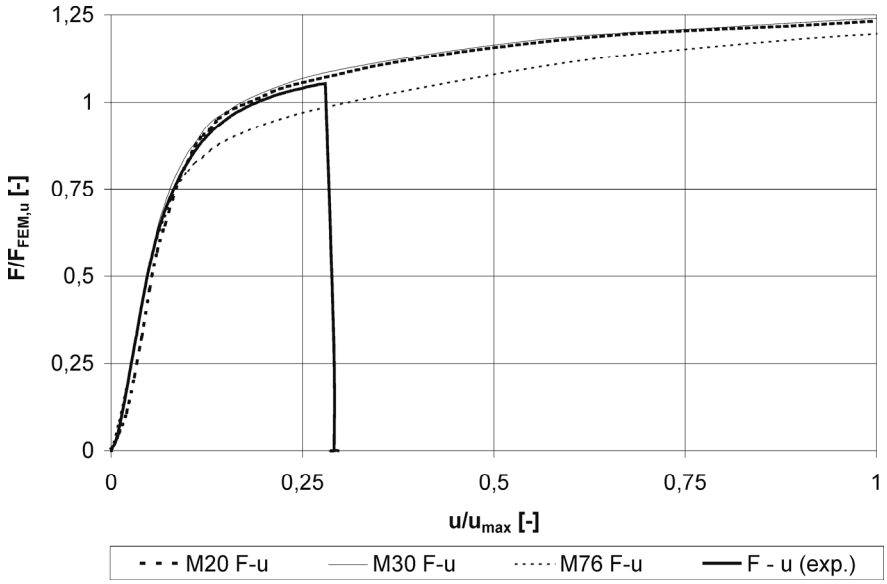

Figure 11. Normalized Load-Displacement-Curves

The normalized load-displacement-curves from the calculations are shown in Figure 11. The displacements are normalized with respect to a maximum translation specified as one fifth of the hole diameter K and the forces are normalized with respect to the ultimate failure load $F_{FEM,u}$. Figure 11 includes a load-displacement-curve obtained experimentally. All of the four curves are in good agreement. The results of the verification show, that

- the load bearing capacity of the tension rod system is modelled physically correct
- the application of the failure criterion leads to a safe and economic estimation of the ultimate failure load

4.5 Results and Comparison of Results

The ultimate failure load of the fork end connectors with pin is calculated with the nominal material properties transformed by Eq. 4 and Eq. 5. It is determined for each size with the failure criterion Eq. 6. Additional calculations are performed with sizes M20, M36 and M76. The ultimate failure loads $F_{FEM,u}$ obtained from the virtual tests and the resistances calculated according to Eq. 1 to Eq. 3 are listed in Table 4 as well as the characteristic resistance $F_{VDI,c}$ of the threaded connection according to VDI-Richtlinie [12].

The load bearing capacity F_{trsys} of the fork end connector with pin is obtained as minimum from $F_{VDI,c}$ and $F_{FEM,u}$. All possible failure modes are included through this.

The results should show that the tension rod governs the load bearing capacity of the system in design. Therefore the ratio η, which is defined as

$$\eta = \frac{\min(F_{FEM,u}, F_{VDI,c})}{\frac{F_{tr,c}}{1{,}1}} \tag{7}$$

has to be greater than the safety factor γ_M specified in DIN 18800-1 [4] or CUAP [6] for this application. The safety factor $\gamma_M = 1.1$, CUAP [6] for tension members is included in the denominator of Eq. 7. The ratios η from the example are given in Table 4. The safety factor γ_M specified in CUAP [6] is $\gamma_M = 1.25$ and in DIN 18800-1 [4] is $\gamma_M = 1.25 \cdot 1.1 = 1.375$. The comparison of η and γ_M shows, that the fork end connectors with sizes M 85, M 90 and M 100 are not determining the load bearing capacity of the tension rod system and thus are not relevant for design.

Table 4. Results of Calculations According to Formulae (1) to (3), VDI-Richtlinie and Results of Virtual Tests

Size		M20	M30	M76	M85	M90	M100
$F_{fce,1,c}$	kN	104	251	2042	2380	2939	3406
$F_{fce,2,c}$	kN	95	214	1745	2132	2555	2994
$F_{fce,3,c}$	kN	161	332	2750	3347	3832	4450
$F_{fce,c}$	kN	95	214	1745	2132	2555	2994
$F_{pin,1,c}$	kN	302	679	4355	6107	6521	8794
$F_{pin,2,c}$	kN	82	209	1146	1810	1838	2799
$F_{pin,c}$	kN	82	209	1146	1810	1838	2799
$F_{tr,1,c}$	kN	124	265	1736	2252	2538	3154
$F_{tr,2,c}$	kN	111	242	1723	2281	2593	3269
$F_{tr,c}$	kN	111	242	1723	2252	2538	3154
$F_{VDI,c}$	kN	204	429	2846	3555	4031	4947
$F_{FEM,u}$	kN	216	388	3366	4230	5027	5761
F_{trsys}	kN	204	388	2846	3555	4031	4947
η	-	2,02	1,77	1,82	1,74	1,75	1,73

5. SUMMARY

The design methods for tension rod systems are presented and discussed. It is shown, that the common design procedures give uneconomic results. Therefore it is advisable to determine the real load bearing capacity by tests. This requires a technical approval. The procedure of testing is time and cost intensive. Costs and duration can be decreased by the application of virtual tests. A general strategy is presented for planning and performing virtual tests. The procedure is divided into several steps. With respect to a physical reasonable and preferably simple numerical model, a thorough consideration of the structure is absolutely necessary. We recommend to divide the component or structure into sub models for the analysis of different failure modes. This allows a target-oriented fine mesh of the individual numerical model for each failure mode and a clear interpretation of the results. All steps of the strategy are explained by the example of an extension of an existing technical approval for a tension rod system.

It has to be kept in mind that virtual tests will only lead to safe results if they are based on a profound knowledge of the load transfer and the possible failure modes. This demands substantial experience with experimental and numerical analysis of the object.

REFERENCES

[1] Kathage, K., Ruf, D.C. and Ummenhofer, T., "Zugstäbe und ihre Anschlüsse", In: Kuhlmann, U. (Editor), Stahlbau-Kalender 2005, Verlag Ernst & Sohn, 2006, pp. 725-784.
[2] EN 1993-1-1:2005-07: Eurocode 3: Design of Steel Structures – Part 1-1: General Rules and Rules for Buildings.
[3] EN 1993-1-8:2005-07: Eurocode 3: Design of Steel Structures – Part 1-8: Design of Joints.
[4] DIN 18800-1:1990-11: Stahlbauten – Bemessung und Konstruktion.
[5] Anpassungsrichtlinie Stahlbau Fassung Dezember 1998, inkl. Änderungen und Ergänzungen Ausgabe Dezember 2001, DIBt Mitteilungen 2002. Sonderheft 11.
[6] CUAP (Common Understanding of Assessment Procedure), "Tension Rod System", Deutsches Institut für Bautechnik, Berlin, 2003.
[7] "Gemeinsame Erklärung des CSTB und DIBt zur technischen Bewertung von Bauprodukten auf Grundlage virtueller Versuche mit dem Ziel der Kostenreduzierung im Bauwesen", DIBt Mitteilungen, 2004, Vol. 35, No. 5, pp. 146-147.
[8] Breitschaft, G. and Häusler, V., "Verwendung von rechnerischen Nachweisen bei Erteilung von Zulassungen", DIBt Mitteilungen, 2004, Vol. 35, No. 5, pp. 147-149.
[9] Kathage, K., "Finite-Elemente-Berechnungen als Grundlage zur Erteilung von Zulassungen für Zugstabsysteme", DIBt Mitteilungen, 2004, Vol. 35, No. 5, pp. 149-151.
[10] Saal, H. and Gehring, A., Gutachten Nr. 044074: Änderung und Ergänzung der bauaufsichtlichen Zulassung Z-14.4-427", Versuchsanstalt für Stahl, Holz und Steine, Universität Karlsruhe (TH), 2004, Unpublished.
[11] Allgemeine bauaufsichtliche Zulassung Z-14.4-427, "Zugstabsystem MACALLOY 460", Deutsches Institut für Bautechnik, Berlin, 2004.
[12] VDI-Richtlinie 2230 Blatt 1:2003-02: Systematische Berechnung hochbeanspruchter Schraubenverbindungen - Zylindrische Einschraubenverbindungen.
[13] Saal, H and Bechtold, M., "Zugstäbe und Seile. Vielfalt der Möglichkeiten? Gestaltung und Nachweis", In: Proceeding of 25th Stahlbauseminar Neu-Ulm, Biberach, 2003.
[14] ABAQUS/Standard. Version 6.4.1. Copyright 2003. ABAQUS, Inc.
[15] ABAQUS Documentation – Version 6.4. Copyright 2003. ABAQUS, Inc.